Phenoxazinone synthase activity of two iron(III) complexes comprising the same Schiff base ligand: Biomimetic functional model and mechanistic investigation

Sourav Chatterjee, Dipankar Sukul, Priyabrata Banerjee, Jaydeep Adhikary

PII: S0020-1693(17)31749-8
DOI: https://doi.org/10.1016/j.ica.2018.01.024
Reference: ICA 18098

To appear in: *Inorganica Chimica Acta*

Received Date: 14 November 2017
Revised Date: 20 January 2018
Accepted Date: 23 January 2018

Please cite this article as: S. Chatterjee, D. Sukul, P. Banerjee, J. Adhikary, Phenoxazinone synthase activity of two iron(III) complexes comprising the same Schiff base ligand: Biomimetic functional model and mechanistic investigation, *Inorganica Chimica Acta* (2018), doi: https://doi.org/10.1016/j.ica.2018.01.024

'Revised'

Old title: Phenoxazinone synthase activity of di and polynuclear iron(III) complexes of analogous Schiff base ligand: Biomimetic functional model and mechanistic investigation

New title: Phenoxazinone synthase activity of two iron(III) complexes comprising the same Schiff base ligand: Biomimetic functional model and mechanistic investigation

Sourav Chatterjee[a], Dipankar Sukul[b], Priyabrata Banerjee[c], Jaydeep Adhikary [d,e,*]

[a] *Department of Chemistry, Panchakot Mahavidyalaya, Sarbari, Purulia, Pin-723121, India*

[b] *Department of Chemistry, National Institute of Technology Durgapur, Durgapur 713 209, India*

[c] *Department of Surface Engineering and Tribology, CSIR-CMERI, Durgapur 713 209, India*

[d] *Department of Chemistry, University of Calcutta, 92 A. P. C. Road, Kolkata-700 009, India*

[e] *Department of Chemical Sciences, Ariel University, Ariel 40700, Israel*

Corresponding author:

E-mail address: adhikaryj86@gmail.com (J. Adhikary).

ABSTRACT

A new 4,4′-bipyridine (4,4′-byp) mediated 1D- polymeric Fe^{III} complex (complex **1**) of Schiff base ligand H_2L, a 1:2 condensation product of 1,2-diaminopropane and salicylaldehyde, has been synthesized. Complex **1** is structurally characterized by single crystal X-ray diffraction. A phenoxo bridged dinuclear Fe^{III} complex (complex **2**) of analogous ligand has been synthesized also. Dioxygen activation in terms of Phenoxazinone synthase activity using *o*-aminophenol (OAPH) as a model substrate catalyzed by both the complexes are thoroughly investigated here. ESI-MS spectral study reveals that polynuclear complex **1** dissociates into mononuclear units while dissolve in methanol during catalytic study. The kinetic study illustrates that both the complexes have well competence towards *o*-aminophenol oxidation where dinuclear Fe^{III} species demonstrate higher activity than mononuclear intermediate species. Important finding from the

mass spectral and electrochemical study provide significant information of the mechanistic pathway of the functioning phenoxazinone synthase like activity of synthesized iron complexes.

1. Introduction

Schiff bases are significant ligands and can be facilely synthesized and coordinated with a series of metal ions. Transition-metal complexes consisting Schiff-base ligands has become one of the most extensively studied topics in coordination chemistry now a days[1] due to ease of synthesis, wonderful structural diversities, and potential applications in diverse fields such as catalysis, medicinal chemistry and material sciences etc. [2]. In recent years, Schiff base type ligands are extensively used to prepare synthetic analogues of metallobiosites such as galactose oxidase, cytochrome P-450, phenoxazinone synthase, catechol oxidase, phosphatase, supper oxide dismutase, urease and many others [3]. Our group has been continuously affianced in studying Schiff-base complexes of transition and post transition metal ions mainly as small synthetic analogs of various metalloenzyme like phosphatase, catechol oxidase and cytochrome P-450 [4]. However, being exceptionally important enzyme, phenoxazinone synthase like activity has not been investigated yet in our group. Multicopper oxidase phenoxazinone synthase is naturally found enzyme in *Streptomyces antibioticus*. This enzyme catalyzes the oxidative dimerization of two molecules of a wide varieties of substituted 2-aminophenol to the phenoxazinone chromophore during the biosynthesis of actinomycin D. This naturally occurring antibiotic is used clinically for the treatment of specific tumors [5]. On the other hand, it is well known that *o*-aminophenol is rapidly metabolized to 2-aminophenoxazine-3-one in human erythrocytes, where oxy and methemoglobin are involved [6]. Thus, it seems that iron containing enzymes can also promote the oxidative dimerization of 2-aminophenol. Therefore, in the present study Fe^{III} Schiff base complexes have been selected for metalloenzyme mimicking of phenoxazinone synthase. In particular, iron complexes of tetradentate Schiff base ligands have been taken under consideration since they exhibit significant catalytic activity, magnetic properties, and unique coordination chemistry [7]. Only a few examples have been found for which iron complexes were used as synthetic analogue of phenoxazinone synthase [8] and no poly nuclear Fe^{III} Schiff base complex has been explored in phenoxazinone synthase like activity till date. Consequently, we have synthesized 4,4′-bipyridine mediated poly nuclear Fe^{III} complex

(complex **1**) and phenoxo bridged dinuclear (complex **2**) of a tetradentate Schiff base ligand (H_2L) (**Scheme 1**). Nevertheless, ESI mass spectrum reflects that the polymeric complex breaks down into mononuclear units during the dissolution of complex **1** in methanol before catalytic study. Both the complexes are capable to oxidize *o*-aminophenol. Detailed mechanistic study has been investigated using cyclic voltammetry and electrospray ionization mass spectral study. Finally, a comparison of the activity of our synthesized iron complexes to the previously reported catalysts strongly suggests that our complexes have excellent catalytic efficiency towards phenoxazinone synthase like activity.

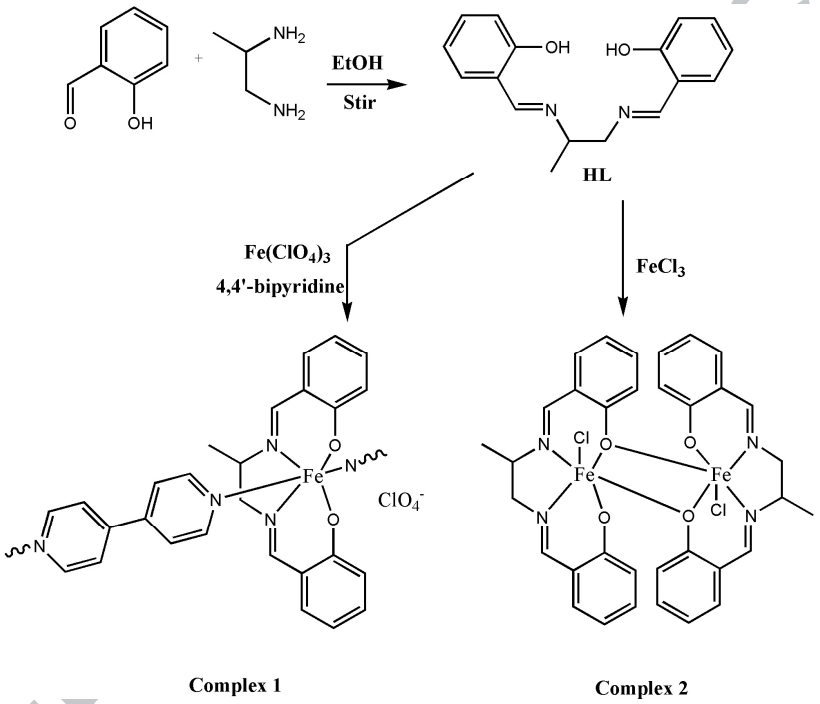

Scheme 1 Synthetic route of complexes **1** and **2.**

2. Experimental Section

2.1. Materials &Methods

All chemicals were obtained from commercial sources and used as received. Solvents were dried according to standard procedure and distilled prior to use.

Elemental analyses were achieved using a Perkin-Elmer 240C elemental analyzer. Fourier-transform infrared spectroscopy (FT-IR) (4000–500 cm^{-1}) data were taken at 27°C using a Perkin-Elmer RXI FT-IR spectrophotometer with KBr pellets. Electronic spectra (900–200 nm) were recorded using a Shimadzu UV-3101PC at 27°C with methanol as solvent and reference. The electrospray ionization mass spectra (ESI-MS) were recorded on a MICROMASS Q-TOF

mass spectrometer. The cyclic voltammetric measurements were performed in dry methanol solutions with 0.2M TBAP as supporting electrolyte (scan rate = 10 mVs^{-1}) employing a PAR potentiostat/ galvanostat model Versa Stat-II. A three-electrode system was used here in which the counter and working electrodes were platinum foils and the reference electrode was a saturated calomel electrode.

2.2. Syntheses

*2.2.1. Synthesis of [{FeL(4,4′-byp)ClO_4}]$_n$(**1**)*

An ethanolic solution (5 mL) of 1,2-diaminopropane (0.109 g, 1 mmol) was added dropwise to ethanolic solution (10 mL) of salicylaldehyde (0.244 g, 2 mmol) and the resulting mixture was stirred for half an hour. Then, an ethanolic solution (10 mL) of iron(III) perchlorate (0.354 g, 1 mmol) was added under continuous stirring condition and followed by the addition of 5mL ethanolic solution of 4 4'-bipyridine (0.156 g, 1 mmol). Resulting solution was then allowed to stir for one hour and filtered. Deep brown colored X-ray suitable square shaped crystals were obtained from the filtrate. Yield: 85%. Anal. Calcd. C, 54.74; H, 4.05; N, 9.46. Found: C, 54.73; H, 4.03; N, 9.44; FTIR: ν(C=N) = 1614 cm^{-1}, ν(skeletal vibration) = 1545cm^{-1}, ν(ClO_4^-) = 1087cm^1; UV–Vis (methanol): 235, 322 and 509 nm.

*2.2.2. Synthesis of [FeLCl]$_2$ (**2**)*

Complex **2** was synthesized following the similar procedure reported by Hai-Liang *et al.*[9]. Yield: 85%. Anal. Calcd. C, 54.89; H, 4.34; N, 7.53. Found: C, 54.83; H, 4.29; N, 7.52; FTIR: ν(C=N) = 1622 cm^{-1}, ν(skeletal vibration) = 1544cm^{-1}; UV–Vis (methanol): 259, 304 and 473 nm.

Caution! Transition metal perchlorate complexes are potentially explosive and should be handled in lesser amounts and with necessary precautions.

2.3. X-ray data collection and structure determination

Diffraction data for complex **1** was collected at room temperature (293 K) on a Bruker Smart CCD diffractometer equipped with graphite monochromated MoKα radiation (λ=0.71073Å). Cell refinement, indexing and scaling of the data set were done using Bruker SMART APEX and Bruker SAINT package [10]. The structure of the complex **1** was solved by

direct methods and subsequent Fourier analyses [11] and refined by the full-matrix least-squares method based on F^2 with all observed reflections using SIR-92 and SHELX-97 [12], software. For the complex, all non-hydrogen atoms were refined with anisotropic thermal parameters and the hydrogen atoms were fixed at their respective positions riding on their carrier atoms and refined anisotropically. All the calculations were made using the WinGX System, Ver 1.80.05 [13], PLATON99 [14], ORTEP3 [15] programs. Selected crystallographic data and refinement details are displayed in **Table 1**.

Table 1 Crystallographic data and details of structure refinement for the complex **1**.

Empirical formula	$C_{27}H_{24}FeN_4O_6Cl$
Formula mass	591.80
Crystal system	Triclinic
Space group	P-1(No. 2)
a (Å)	9.796(2)
b (Å)	11.466(2)
c (Å)	15.055(3)
α (°)	100.231(2)
β (°)	104.842(2)
γ (°)	106.828(2)
V (Å3)	1505.5(5)
Z	2
T (K)	293
μ(MoKα) (/mm)	0.633
Dcalc (Mg/m3)	1.306
F(000)	610
θ max (deg)	24.9
Tot., Uniq. Data, Rint	10105, 5096, 0.024
Observed (I > 2σ(I))	4210
Nref, Npar	5096, 391

R, wR2, S	0.0646, 0.1927, 1.08
residual extrema (e/Å3)	-0.44, 0.63

2.4. Catalytic oxidation of o-aminophenol

Phenoxazinone synthase like activity of our synthesized complexes (**1** and **2**) was investigated by the reaction of 1.0×10^{-4} M methanolic solutions of the complexes with 0.01 M solution of *o*-aminophenol (OAPH) in dioxygen saturated methanol at room temperature. The reaction was monitored spectrophotometrically by monitoring the enhancement of the absorbance as a function of time at ca. 433 nm which is typical band of the phenoxazinone chromophore [16]. Determination of various kinetic parameters for the catalytic activity was carried out by using the same procedure reported earlier [16]. In addition, to confirm the rate dependency on catalyst concentrations similar set of experiments were performed at a fixed concentration of substrate with varying amount of catalyst. Rate of a reaction was estimated from the initial rate method. All measurements were performed in triplicate, and the average values were adopted.

3. Results and discussions

3.1. Syntheses and characterization

Addition of $Fe(ClO_4)_3$ to the ethanolic solution of H_2L followed by the addition of 4,4′-bypiridine afforded complex **1**. The crystal structure was determined by X-ray analysis (*vide infra*). Crystal structure reveals that complex **1** has 1D polymeric structure. Addition of $FeCl_3$ to the ethanolic solution of H_2L provided phenoxo bridged dinuclear Fe^{III} complex (complex **2**). Unfortunately, the crystal structure of **2** was reported by another group [9]. The complexes **1** and **2** were characterized by routine physiochemical analyses. The complexes exhibit characteristic FTIR bands at the range of 1614-1622 cm^{-1} and 1544–1545 cm^{-1}assigned to C=N and skeletal vibrations (**Fig. S1-2**, **Supplementary information**), respectively. Complex **1** also shows broad FTIR band centered in the range of 1068-1087 cm^{-1} due to presence of the perchlorate ion [16b]. The electronic spectra for **1** and **2** in methanol show a band at 473-509 nm can be assigned as charge-transfer transitions from the in-plane pπ orbital of the phenolate to the half-filled dπ* orbital of iron(III) (**Fig. S3**, **Supplementary information**). Other two electronic spectral bands

at ~235-259 and ~304-322 nm can be attributed to π-π* and ligand to metal charge transfer (LMCT) transitions, respectively, as reported earlier [3e].

*3.2. Description of structure of complex **1***

The perspective view of the monomeric unit of complex **1** is illustrated in **Fig. 1**. The structure consists of distorted octahedral iron(III) center coordinated equatorially by the ictetradentate Schiff base ligand which provides a N_2O_2 donor set. The $[Fe(III)(salen)]^+$ moieties are then bridged by the two connecting 4,4′-bipyridyl ligand, to form infinite 1-D chain (**Fig. 2**). Each $[Fe(III)(salen)]^+$ species is neutralized by one perchlorate counter anion which is not involved in polymerization. Selected bond lengths and angles of complex **1** are depicted in **Table 2**. The Fe(1)-O(1) and Fe(1)-O(2) bond distances are found to be 1.886(3) and 1.889(3) Å, and are very similar with those of related iron(III)(salen) compounds which are in the range from 1.887(6) to 1.894(7)Å with pertaining to the phenoxy axial ligand [17-19]. The Fe(1)-N(1) and Fe(1)-N(2) bond distances are found to be 2.092(5) and 2.094(4)Å, which are similar to those observed in related Fe(salen) type compound [20]. Axial positions of metal center are occupied by N atoms of two 4,4′-bipyridyl groups having Fe(1)-N(3) and Fe(1)-N(4) bond distances are 2.205(4) and 2.230(4), respectively. Successive Fe…Fe distance is 11.466 Å.

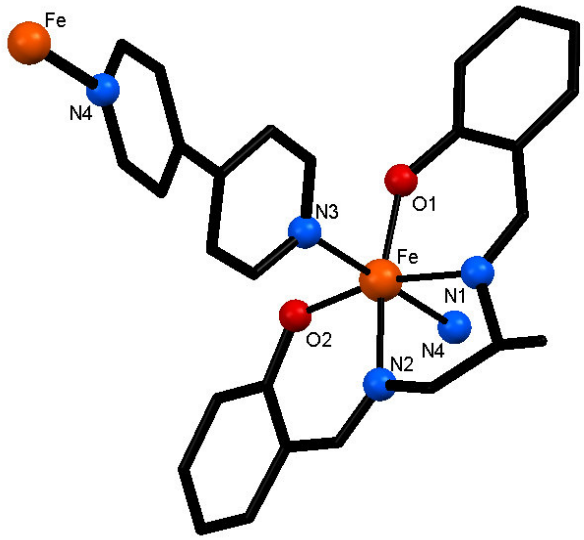

Fig. 1 Crystal structure of complex **1**. Hydrogen and perchlorate anion are omitted for clarity.

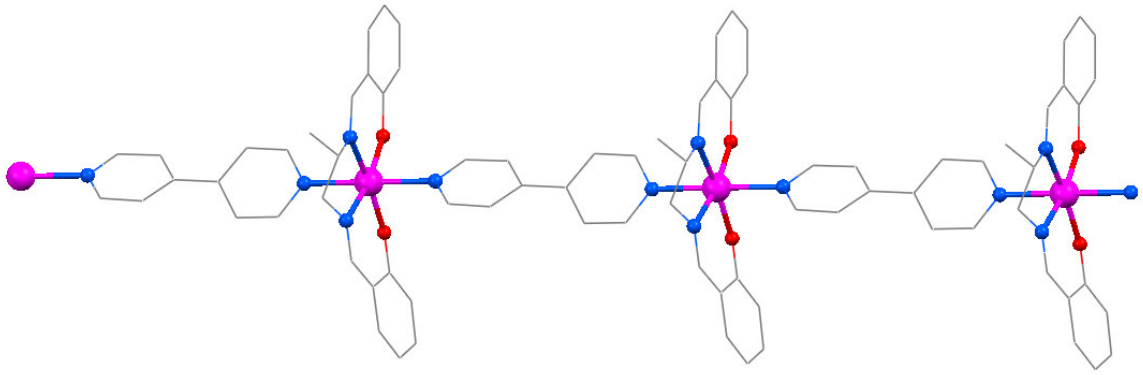

Fig. 2 Representation of 1D polymeric chain of complex **1**. Hydrogen atoms and distorted perchlorate anions are omitted for clarity.

Table 2 Selected bond distances (Å) and angles (°) for the complex **1.**

Fe -O1	1.886(3)	O1-Fe-O2	106.25(13)
Fe -O2	1.889(3)	O1-Fe -N1	89.11(16)
Fe -N1	2.092(5)	O1-Fe -N2	165.54(17)
Fe -N2	2.094(4)	O1-Fe -N3	89.08(15)
Fe -N3	2.205(4)	O1-Fe -N4	89.72(14)
Fe -N4	2.230(4)	O2-Fe-N1	164.31(16)
		O2-Fe-N2	88.12(16)
		O2-Fe-N3	91.12(15)
		O2-Fe-N4	87.07(14)
		N1-Fe -N2	76.65(19)
		N1-Fe -N3	92.37(19)
		N1-Fe -N4	89.84(18)
		N2-Fe -N3	89.04(17)
		N2-Fe-N4	92.67(15)
		N3-Fe-N4	177.46(14)

3.3. Phenoxazinone synthase like activity

Catalytic oxidation of *o*-aminophenol (OAPH) was examined spectrophotometrically in dioxygen saturated methanolic solution at room temperature. In order to confirm the ability of our synthesized complexes to oxidize OAPH, 1.0×10^{-4} M methanolic solutions of the complexes were treated with a 1×10^{-2} M (100 equiv) of OAPH under aerobic conditions. The catalytic studies were performed in the absence of any added base to minimize the possibility of auto oxidation of OAPH. The course of the reaction was followed by UV–Vis spectroscopy, and the time dependent spectral scans of the two complexes are depicted in **Fig. 3** and **4**. The spectral scan reveals the development of peak intensity at ca. 433 nm, characteristic of phenoxazinone chromophore, suggesting the catalytic oxidation of OAPH to 2-aminophenoxazine-3-one in aerobic condition [16]. A blank experiment without catalyst in an identical condition does not show any increment in the band intensity at 433 nm. These spectral behaviors clearly reveal that both the complexes are active catalysts for the aerial oxidation of OAPH to the corresponding phenoxazinone chromophore.

Reaction kinetics was performed to understand the extent of the catalytic efficiency of the complexes. The concentration of OAPH was always kept 10 times higher than that of the complex and the rise of respective 2-aminophenoxazine-3-one concentration were determined at 433 nm wavelength for each complex. Solutions of OAPH of concentration ranging from 0.001 to 0.05 mol dm^{-3} were prepared from a concentrated stock solution in methanol. 2 mL methanolic solution of the substrate were taken in a 1 cm spectrophotometer quartz cell thermostated. 0.04 mL of 0.005 mol dm^{-3} complex solution was then quickly added to it so that the ultimate concentration of the complex becomes 1×10^{-4} mol dm^{-3}. The dependence of the initial rate on the concentration of substrate was spectrophotometrically monitored at 433 nm. The initial rates method shows a first-order dependence on complex concentration and exhibited saturation kinetics at higher substrate concentrations. This type of saturation rate dependency on the concentration of the substrate can be treated with the Michaelis–Menten model, which on linearization gives a double reciprocal Lineweaver–Burk plot to analyze the values of maximum velocity (V_{max}), binding constant (K_M), and rate constant (k_{cat}) (**Fig. S4-S7, Supplementary information**). All these kinetic parameters of both the complexes for OAPH oxidation are demonstrated in **Table 3**. **Table 4** represents the k_{cat} values of *o*-aminophenol oxidation of some transition metal complexes reported in recent years [8,16b,21]. On comparing **Tables 3** and **4** it

may be stated that complexes **1** and **2** belongs to the highly efficient catalysts group where the order of their activity is **2>1**.

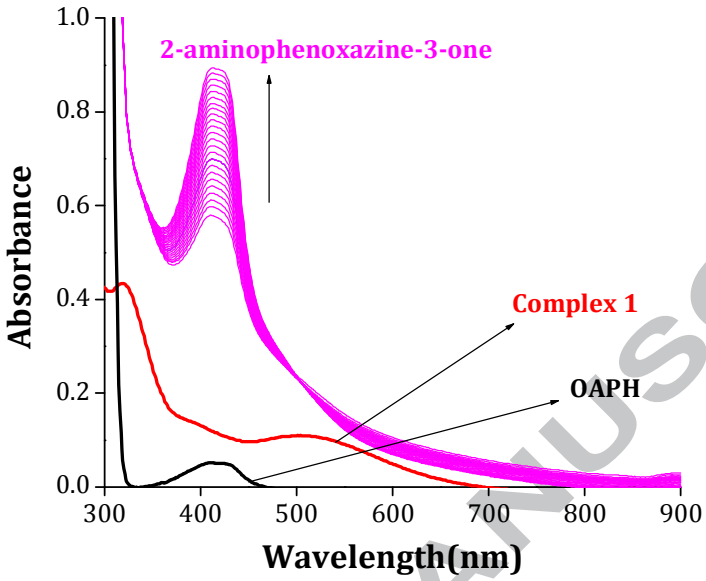

Fig. 3 UV–Vis spectral scans showing the increase in phenoxazinone chromophore band at 422 nm after the addition of o-aminophenol (0.001 M) to a solution of complex **1** (1×10^{-4} M) in methanol at 25°C. The spectra were recorded for the period of 2h.

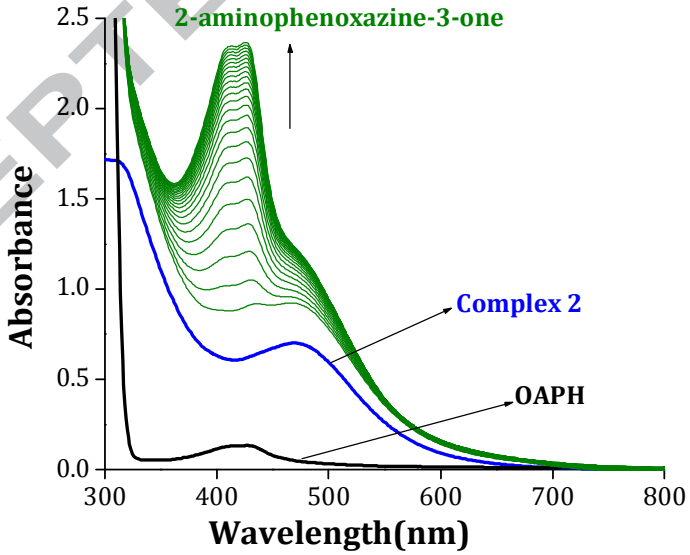

Fig. 4 UV–Vis spectral scans showing the increase in phenoxazinone chromophore band at 422 nm after the addition of o-aminophenol (0.001 M) to a solution of complex **2** (1×10^{-4} M) in methanol at 25°C. The spectra were recorded for the period of 2 h.

Table 3 Kinetic parameters for complex **1** and **2.**

Catalyst	V_{max} (Ms^{-1})	K_M(M)	k_{cat} (h^{-1})
1	8.989×10^{-7}	2.22×10^{-3}	32.36
2	5.449×10^{-6}	8.19×10^{-3}	196.18

Table 4 Kinetic data for phenoxazinone synthase like activity of different metal complexes.

	Catalyst[a]	**Solvent**	k_{cat}**(h^{-1})**	**Ref.**[year]
1.	$[FeCl_2(L^5)]$	DMF	137	8a [2014]
2.	$[Co(L^2)(N_3)_3]$	Methanol	33.26	21a[2014]
3.	$[Co_2(amp)_2(\mu\text{-imp})_2Cl_2]Cl_2\cdot2H_2O$	Methanol	13.75	21b[2013]
4.	$[Co(L^1)Cl(H_2O)]Cl\cdot H_2O$	Methanol	13.68	21c[2013]
5.	$[Mn(L^4)Cl_2]\cdot H_2O$	Methanol	26.32	21d[2013]
6.	$[Fe(L^1)Cl_3]$	Methanol	56	8b[2012]
7.	$[Mn(6'Me_2indH)(H_2O)_2(CH_3CN)](ClO_4)_2$	DMF	2.93	21e[2008]
8.	$[Mn(Br_4Cat)(Br_3pyCat)(py)_2]$	DMF	22.39	21f[2016]
9.	$[Mn(HL)_2](ClO4)_2$	Methanol	138.62	16b[2016]
10.	$[LCo(L')_2]ClO_4$	Methanol	11.48	21g[2016]
11.	$[Co(L)(N_3)_2]$	Methanol	54.0	21h[2017]

[a](1) [HL^5 =1,3-bis(5′-methyl-2′-thiazolylimino)isoindoline]; (2)[L^2=(2-pyridylmethyl)(2-pyridylethyl)amine]; (3) [amp = 2-aminomethylpyridine; imp = 2-iminomethylpyridine anion]; (4) [L^1=N,N′-bis(pyridin-2-ylmethylene)-2,2-dimethylpropane-1,3-diamine]; (5)[L^4=hexahydro-1-(2-(tetrahydro-2-(pyridin-2-yl)pyrimidin-(2H)-yl)ethyl)-2-(pyridin-2-yl)pyrimidine]; (6) [L^1=N,N′-Bis(2-Methylbenzimidazolyl) pyridinediamide]; (7) [6′Me_2indH= 1,3-bis(6′-methyl-2′-pyridylimino)isoindoline]; (8) py = pyridine, Br_4CatH_2 = tetrabromocatechol and $Br_3pyCatH_2$ = 3,5,6-tribromo-4-pyridiniumcatechol; (9) LH = 4-*tert*-butyl-2,6-bis-[(2-pyridin-2-yl-ethylimino)-methyl]-phenol; (10) L'=4-aminopyridine, H_2L= N,N'-bis(3-

methoxysalicylidehydene)cyclohexane-1,2-diamine; (11) HL= 2-{[3-(3-Dimethylamino-propylamino)-propylimino]-methyl}-6-methoxy-phenol.

3.4. Electrochemical study

It is very essential to check the electrochemical behavior of biomimetic models since the redox potential of the active site of a metalloenzyme plays a vital role in catalyzing the oxidation of various organic matters. The electrochemical features of the two complexes were investigated in methanol solution by employing cyclic voltammetry (CV) stationary platinum-sphere electrode. Typical cyclic voltammogram of two complexes are depicted in **Fig. 5**. Electrochemical data for complexes are tabulated in **Table 5**. The cyclic voltammogram of the complexes **1–2** exhibit redox waves at negative potentials that can be assigned to a Fe^{III}/Fe^{II} redox couple [22,23]. Two complexes exhibit a cathodic (-0.185 to -0.403 V) as well as an anodic wave (-0.083 to -0.265V). The values of the peak current ratio (i_{pa}/i_{pc}), which is far from unity, and the peak potential separation (ΔEp, 103–138 mV) clearly reveal that the redox process is far from reversible. The $E_{1/2}$ values of Fe^{III}/Fe^{II} redox potentials follow the trend **2** > **1**, reflecting a decrease in Lewis acidity of the iron(III) center of **1** from **2**.

It is already demonstrated that the rate of OAPH oxidation of complex **2** is much higher than complex **1**. This fact is now also supported by the electrochemical data that the reduction of complex **1** is quite difficult as compared to **2** as $E_{1/2}$ value of $Fe^{III} \rightarrow Fe^{II}$ process for complex **1** is more negative than that of **2**. Consequently, the effectivity towards *o*-aminophenol oxidation is higher for complex **2**.

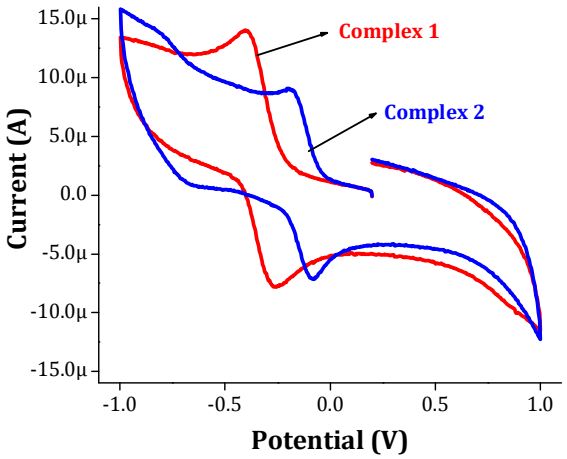

Fig. 5 Cyclic voltammograms (CV) of the complexes in methanol solution at 25°C. Supporting electrolyte: 0.1 M TBAP. Scan rate: 50 mV s^{-1}.

Table 5 Electrochemical data of the complexes in methanol at 25°C.

Complex	$E_{p,a}$(V)	$E_{p,c}$(V)	ΔE_p(V)	$E_{1/2}$(V)	Redox Process
1	-0.265	-0.403	0.138	-0.334	$Fe^{III} \rightarrow Fe^{II}$
2	-0.083	-0.185	0.102	-0.134	$Fe^{III} \rightarrow Fe^{II}$

3.5. Electrospray ionization mass spectral study

The electrospray ionization mass spectra (ESI-MS positive) of compounds **1** and **2** were recorded in methanol solution and are depicted in **Fig. S8** and **S9(Supplementary information)**, respectively. Compound **1** exhibits two assignable peaks at m/z = 336.0352 (base peak) and 689.1639 with line-to-line separation of 1.0 corresponds to $[FeL]^+$ and $[ArFeL(4,4'\text{-byp})_2]^+$, respectively. The spectrum clearly implies that polymeric moiety dissociates into mononuclear units in methanol. Complex **2** has also two peaks at m/z = 336.1289 (base peak) and 707.0813 can be assigned as $[FeL]^+$ and $[\{FeL\}_2\text{-}Cl]^+$, respectively [line-to-line separation of 1.0]. The result clearly tells that the base peaks in both complexes are same. However, the rate of *o*-aminophenol oxidation of both complexes are different, indicating that the active species for two complexes are not the identical. In order to find a perception into the nature of plausible complex–substrate intermediates, the ESI-MS positive spectra of a 1: 50 mixture of the complexes and *o*-aminophenol in methanol were recorded after 10 minutes of their mixing. The spectrum for the compound **2** (most active) is depicted in **Fig. 6** and **S10 (Supplementary information)**. The peaks at 780.1573 and 467.0909 with line-to-line separation of 1.0 can be assigned as $[\{Fe^{III}L\}_2\text{-}(OAP)]^+$ and $[Fe^{III}L\text{-}(OAP)Na]^+$, respectively. The peak at m/z = 213.1001 can be described to the protonated species of 2-aminophenoxazine-3-one. Base peak at m/z = 336.0561 is already assigned as $[FeL]^+$. The remaining peaks at m/z = 672.1124 and 358.8539 are most interesting and can be assigned as $[Fe^{III}\ Fe^{II}L_2]^+$ and $[Fe^{II}L\text{-}Na]^+$, respectively. These interesting peaks are absent in case of the ESI-MS spectra of sole complex and thus definitely these species can only generate due to reduction of iron(III) center during the OAPH oxidation. The ESI-MS positive spectra of a 1: 50 mixture of the complex **1** and *o*-aminophenol in methanol

recorded after 10 minutes of mixing is depicted in **Fig. S11** (**Supplementary information**). The spectrum exhibits 4 peaks at m/z = 335.9214(base peak), 213.1018, 358.9010 and 466.9208 with line-to-line separation of 1.0. All those peaks are already assigned before. Peak at m/z = 358.9010 is generated during the oxidation process as happened in case of complex **2**. The experimental and the simulated spectral patterns are in nice agreement with each other, demonstrating accurate assignment of the species. During the oxidation process for both complexes one common intermediate, namely $[Fe^{III}L\text{-}(OAP)Na]^+$, was formed but $[\{Fe^{III}L\}_2\text{-}(OAP)]^+$ was only generated in case of complex **2**. And probably this unique intermediate promotes complex **2** to show higher activity of complex **2** over **1** towards OAPH oxidation.

With the help of some relevant references [8b,21a] and the ESI-MS spectral data, we have proposed a plausible mechanistic pathway of phenoxazinone synthase like activity of the most active complex **2** (**Scheme 2**).

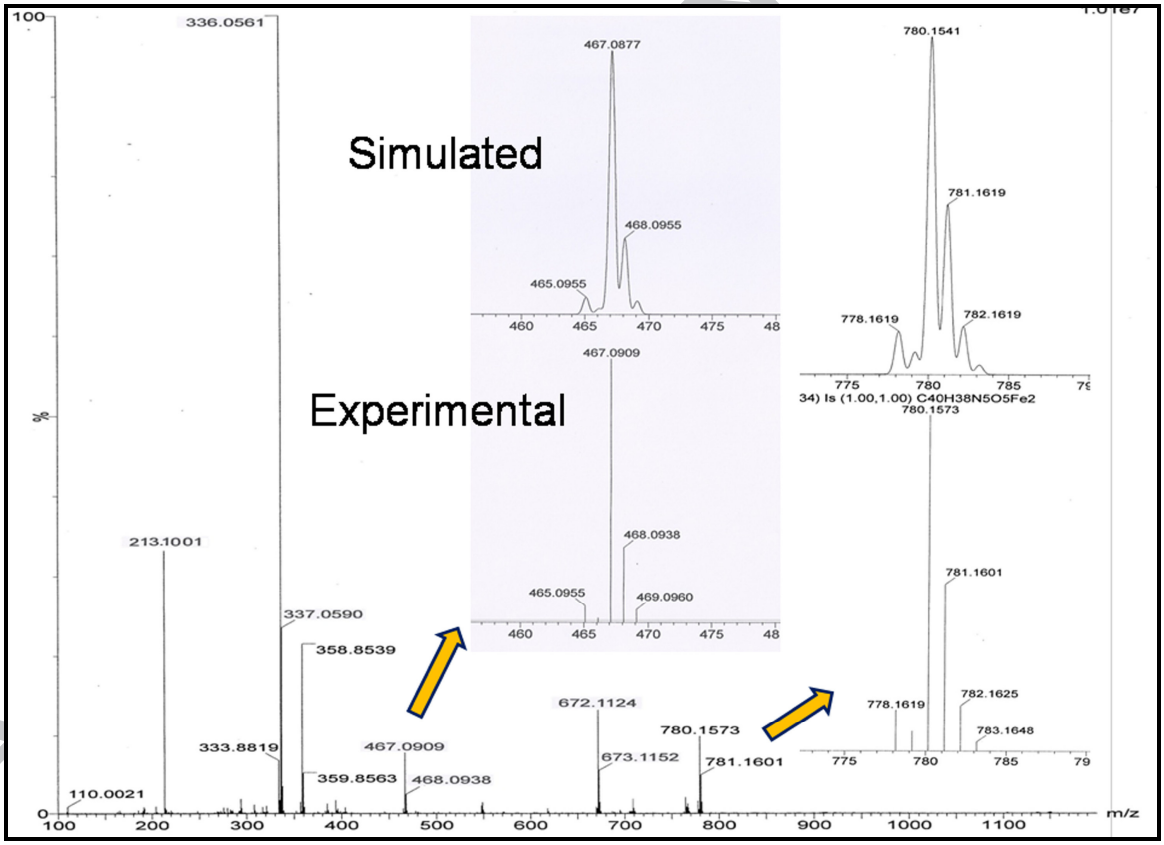

Fig. 6 Electrospray ionization mass spectrum (ESI-MS positive) of a 1: 50 mixture of complex **2** and o-aminophenol in methanol recorded after 10 min of mixing, showing experimental and simulated isotopic distribution patterns.

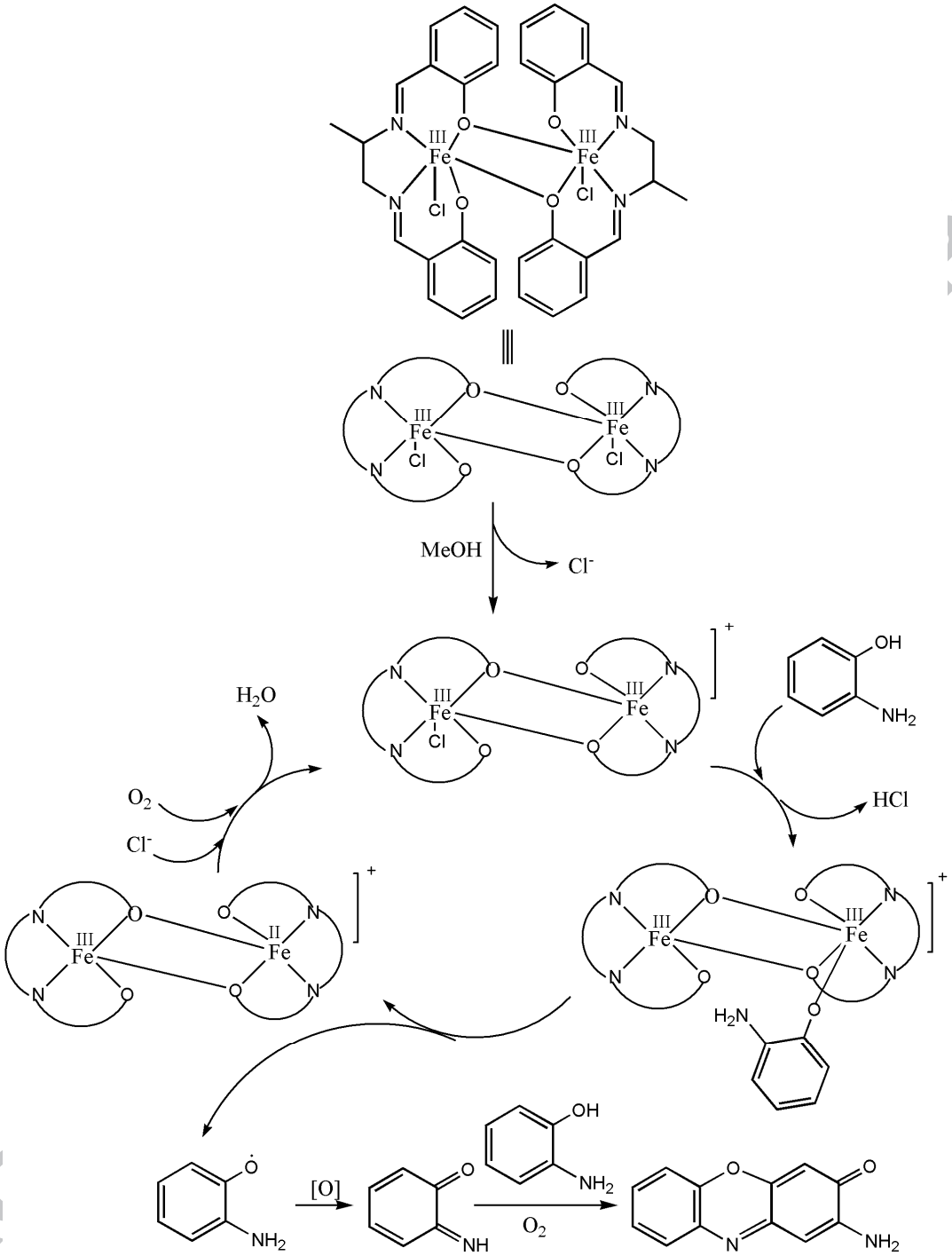

Fig. 7 Plausible mechanistic pathway showing the formation of 2-aminophenoxazine-3-one in which complex **2** chosen as model complex.

4. Conclusions

In summary, our study expresses the syntheses and characterization of one polymeric and one dinulcear Fe^{III} complexes of a ONNO donor Schiff base ligand. The complexes are efficient

catalysts for the 2-aminophenol oxidation, which means that the examined systems serve as functional models for phenoxazinone synthase enzyme. The ESI-MS positive spectra together with UV-vis spectroscopy clearly suggest the formation of a catalyst–substrate adduct by a substitution reaction in the catalytic cycle. Higher efficiency of dinuclear iron complex over the mononuclear species towards the *o*-aminophenol oxidation process has been elucidated by the electrochemical and ESI-MS study. Low negative value of reduction potential and generation of higher number of active species during catalytic process are the reason for higher activity of complex **2**. On the other hand, high negative reduction potential and rigid structure content of the complex **1** are jointly responsible for the lower activity of 4,4'-bipyridine coordinated complex.

Acknowledgements

The author (J.A) gratefully acknowledge Prof. Debasis Das of University of Calcutta, India for his valuable suggestions.

Appendix A. Supplementary data

CCDC 1025941 contains the supplementary crystallographic data for the complex 1 reported in this paper. These data can be obtained free of charge from the Cambridge Crystallographic Data Centre via www.ccdc.cam.ac.uk/data_request/cif. Supplementary data associated with this article can be found in the online version, at doi:XXXX.

References

[1] (a) S. W. Kwak, B.H. Choi, J.H. Lee, H. Hwang, J. Lee, H. Kwon, Y. Chung, K.M. Lee, M. H. Park, Inorg. Chem. 56(2017)6039; (b) P. Mahapatra, S. Ghosh, S. Giri, V. Rane, R. Kadam, M. G. B. Drew, A. Ghosh, Inorg. Chem. 56(2017)5105; (c) T. Yoshimura, M. Nakaguchi, K. Morimoto, Inorg. Chem. 56(2017)4057; (d) P. Ghorai, A. Dey, P. Brandão, J. Ortega-Castro, A. Bauza, A. Frontera, P. P. Ray, A. Saha, Dalton Trans. 46(2017)13531; (e) S. Roy, M. G. B. Drew, A. Bauzá, A. Frontera, S. Chattopadhyay, Dalton Trans. 46(2017)5384; (f) A.K. Ghosh, M. Mitra, A. Fathima, H. Yadav, A. R. Choudhury, B.U. Nair, R. Ghosh, Polyhedron 107(2016)1; (g) S. J. Kirubavathy, S. Chitra, J. Mol. Struc.

1147(2017)797; (h) L. Pogány, J. Moncol, M. Gál, I. Šalitroš, R. Boča, Inorg. Chim. Acta 462(2017)23.

[2] (a) C. P. Pradeep, S. K. Das, Coord. Chem. Rev. 257(2013)1699; (b) K.C. Gupta, A. K. Sutar, C.C. Lin, Coord. Chem. Rev. 253(2009)1926; (c) E. L. Gavey, M. Pilkington, Coord. Chem. Rev. 296(2015)125; (d) R. M. Clarke, K. Herasymchuk, T. Storr, Coord. Chem. Rev. 352(2017)67.

[3] (a) S. Bosch, P. Comba, L. R. Gahan, and G. Schenk, Inorg. Chem. 53(2014)9036; (b) S. Anbu, S. Kamalraj, B. Varghese, J. Muthumary, M. Kandaswamy, Inorg. Chem. 51(2012) 5580; (c) H. Arora, S. K. Barman, F. Lloret, R. Mukherjee, Inorg. Chem. 51(2012) 5539; (d) V. K. Bhardwaj, A. Singh, Inorg. Chem. 53(2014)10731. (e) J. Adhikary, A.Datta, S.Dasgupta, A.Chakraborty, M. I. Menéndez, T. Chattopadhyay, RSC Adv.5(2015)92634; (f) A. Panja, RSC Adv. 4(2014)37085.

[4] (a) K.S. Banu, T. Chattopadhyay, A. Banerjee, S. Bhattacharaya, E. Suresh, M. Nethaji, E. Zangrando, D. Das, Inorg. Chem.47(2008)7083; (b) T. Chattopadhyay, M. Mukherjee, A. Mondal, P. Maiti, A. Banerjee, K.S. Banu, S. Bhattacharya, B. Roy, D.J. Chattopadhyay, T.K. Mondal, M. Nethaji, E. Zangrando, D. Das, Inorg. Chem. 49(2010)3121; (c) J. Adhikary, A. Guha, T. Chattopadhyay and D. Das, Inorg. Chim. Acta 406(2013)1; (d) T. Ghosh, J. Adhikary, P. Chakraborty, P.K. Sukul, M.S. Jana, T.K. Mondal, E. Zangrando, D. Das, Dalton Trans. 43(2014)841; (g) J. Adhikary, P. Chakraborty, S. Das, T. Chattopadhyay, A. Bauz´a, S. K. Chattopadhyay, B. Ghosh, F. A. Mautner, A. Frontera, D. Das, Inorg. Chem. 52(2013)13442; (h) P. Chakraborty, J. Adhikary, B. Ghosh, R. Sanyal, S. K. Chattopadhyay, A. Bauza, A. Frontera, E. Zangrando, D. Das, Inorg. Chem. 53(2014)8257; (i) R. Sanyal, X. Zhang, P. Kundu, T. Chattopadhyay, C. Zhao, F. A. Mautner, D. Das, Inorg. Chem. 54(2015)2315.

[5] E. Frei, Cancer Chemother. Rep. 58 (1974) 49; U. Hollstein, Chem. Rev. 74 (1974) 625.

[6] [(a)A. Tomoda, J. Yamaguchi, H. Kojima, H. Amemiya, FEBS Lett. 196 (1986) 44; (b) M. Wind, A. Stern, Experientia 33 (1977) 1500; (c) H.T. Nagasawa, H.R. Gutmann, M.A. Morgan, J. Biol. Chem. 234 (1959) 1600.

[7] (a) E. Y. Tshuva, S. J. Lippard, Chem. Rev. 104(2004)987; (b) C. Benelli, D. Gatteschi, Chem. Rev. 102(2002)2369; (c) G. H. Spikes, E. Bill, T. Weyhermuller, K. Wieghardt, Chem. Commun. (2007)4339.

[8] (a) M. Szávuly, R. Csonka, G. Speier, R. Barabás, M. Giorgi, J. Kaizer, J. Mol. Catal. A: Chem. 392(2014)120; (b) R.Bakshi, R. Kumar, P. Mathur, Cat.Comm. 17(2012)140; (c) A. Panja, Polyhedron 43 (2012)22.

[9] Z-L You, H-L Zhu, Acta Crystallogr. Sect. E: Struct. Rep.Online, 2004, 60, m1046.

[10] Bruker, SMART, SAINT. Software Reference Manual Bruker AXS Inc. Madison, Wisconsin, USA, 2000.

[11] G. M. Sheldrick, Acta. Crystallogr. Sect A, 64(2008)112.

[12] G. M. Sheldrick, SHELXL 97, Program for the Refinement of Crystal Structures, University of Gottingen, Germany, 1997.

[13] L. J. Farrugia, J. Appl. Crystallogr. 32(1999)837.

[14] A. L. Spek, PLATON, Molecular Geometry Program, University of Utrecht, The Netherlands, 1999.

[15] L. J. Farrugia, J. Appl. Cryt. 30(1997)565.

[16] (a) C. Mukherjee, T. Weyhermuller, E. Bothe, E. Rentschler, P. Chaudhuri, Inorg. Chem. 46(2007)9895; (b) J. Adhikary, A. Chakraborty, S. Dasgupta, S. K. Chattopadhyay, R. Kruszynski, A. Trzesowska-Kruszynska, S. Stepanović, M. Gruden-Pavlović, M. Swart, D. Das, Dalton Trans. 45(2016)12409.

[17] M. Bhadbhade-Mohan, D. Srinivas, Polyhedron 17(1998)2669.

[18] J. Donald, C. Darensbourg, G. Ortiz, R. Billodeaux, Inorg. Chim. Acta 357(2004)2143.

[19] X. Feng J. G. Wang, C. Z. Xie, N. Ma, Z. Anorg. Allg. Chem. (2007)2085.

[20] P. Roy and M. Manassero, Dalton Trans. 39(2010)1539.

[21] (a) A. Panja, M. Shyamal, A. Saha and T.K. Mandal, Dalton Trans. 43(2014)5443; (b) A. Panja, P. Guionneau, Dalton Trans. 42(2013)5068; (c) A. Panja, Polyhedron 80(2014)81; (d) A. Panja Polyhedron 79(2014)258; (e) J. Kaizer, G. Bara´th, R.Csonka, G. Speier, L. Korecz, A. Rockenbauer, L. Pa´rka´nyi, J. Inor. Biochemistry 102(2008)773; (f) A. Panja, N. Ch. Jana, M. Patra, P. Brandão, C. E. Moore, D. M. Eichhorn, A. Frontera, J. Mol. Catal. A: Chem. 412(2016)56; (g) M. Mahato, D. Mondal, and H. P. Nayek,

ChemistrySelect, 1(2016)6777; (h) A. Panja, N. C. Jana, P. Brandão, New J. Chem. 41(2017)9784.

[22] (a) R. Viswanathan, M. Palaniandavar, T. Balasubramanian, P. T. Muthiah, J. Chem. Soc. Dalton Trans. (1996)2519; (b) R. Viswanathan, M. Palaniandavar, T. Balasubramanian, P. T. Muthiah, Inorg. Chem. 37(1998)2943.

[23] M. Velusamy, R. Mayilmurugan, M. Palaniandavar, J. Inorg. Biochem. 99(2005)1032.

Highlights

1) Dinuclear and polynuclear iron(III) complexes of ONNO donor Schiff base ligand have been synthesised and characterised.

2) Phenoxazinone synthase activity of both the complexes was scrutinized thoroughly.

3) Probable mechanistic pathway involved in the catalytic reaction has been proposed with the help of cyclic voltammeter and electrospray ionization mass spectrometer.